

Kinetic process of mechanical alloying in $\text{Fe}_{50}\text{Cu}_{50}$

J. Y. Huang*

*Research Center for Ultrahigh-Voltage Electron Microscopy, Osaka University, Yamada-oka, Suita, Osaka 565, Japan
and Laboratory of Atomic Imaging of Solids, Institute of Metal Research, Chinese Academy of Sciences,
Shenyang 110015, People's Republic of China*

J. Z. Jiang

Department of Physics, Building 307, Technical University of Denmark, DK-2800 Lyngby, Denmark

H. Yasuda and H. Mori

Research Center for Ultrahigh-Voltage Electron Microscopy, Osaka University, Yamada-oka, Suita, Osaka 565, Japan

(Received 13 July 1998; revised manuscript received 3 September 1998)

It is shown that mechanical alloying in the immiscible Fe-Cu system is governed by the atomic shear event and shear-induced diffusion process. We found that an α -to- γ phase transformation, as evidenced by the Nishiyama-Wasserman orientation relationship, occurs by simultaneous shearing process when the grain size reduces to about 20 nm and Cu content reaches 20 at. % in bcc- $\text{Fe}_{\text{rich}}\text{Cu}$ grains in the intermediate stage of milling of $\text{Fe}_{50}\text{Cu}_{50}$. Further milling promotes the interdiffusion between fcc- $\text{Fe}_{\text{rich}}\text{Cu}$ and fcc- $\text{FeCu}_{\text{rich}}$, which is favored because of the similarity of the lattice structures, until a complete fcc Fe-Cu solid solution is formed. The results provide significant insight into the understanding of recent experiments showing that chemical mixing of immiscible elements can be induced by mechanical alloying. [S0163-1829(98)51342-2]

The formation of metastable phases by mechanical alloying (MA) of elemental powder blends has been demonstrated in a variety of alloy systems in recent years.¹ In particular, much work has concentrated on the formation of metastable phases in alloy systems which exhibit a negative heat of mixing of the alloy components and the phase formation has been studied from both the thermodynamic and kinetic viewpoints.² The mechanism of phase formation has been explained by an interdiffusion reaction of the components occurring during the milling process. On the other hand, phase formation in alloy systems with positive heats of mixing is far from being understood from both thermodynamic and kinetic viewpoints, although it has been observed in several systems.³ For example, the phase formation in Fe-Cu system has been extensively investigated by various techniques such as x-ray diffraction (XRD), neutron diffraction, extended x-ray-absorption fine structure (EXAFS), differential scanning calorimetry (DSC), high resolution transmission electron microscopy (HRTEM), Mössbauer spectroscopy, magnetic measurements, etc.⁴⁻¹⁵ On the basis of the results of these measurements, it has been concluded that true alloying at atomic level occurs in the Fe-Cu system during milling.³ It is found that the single fcc- and bcc- $\text{Fe}_x\text{Cu}_{100-x}$ phase regions are largely extended to $x < 60$ at. % and $x > 80$ at. %, respectively,³ despite the equilibrium mutual solid solubilities of less than 0.1 at. % below 600 °C.¹⁶ The mechanism responsible for this significantly enhanced solubility is still a subject of debate. In this work we report an HRTEM study of $\text{Fe}_{50}\text{Cu}_{50}$ specimens in the intermediate stage of milling (i.e., in partly alloyed specimens). The kinetics of the alloying process is discussed on the basis of experimental observations.

Fe (99.9 at. %) and Cu (99.9 at. %) powders with particle sizes smaller than 100 μm were mixed to a desired composition of $\text{Fe}_{50}\text{Cu}_{50}$ and loaded in Ar atmosphere into hardened steel balls and vials in a planetary ball mill (Fritsch Pulverisette 5). The vial was sealed under an Ar atmosphere

to prevent oxidation of both the Fe and Cu powders. After milling for several hours, pallet agglomerates of about 0.7 mm in diameter and about 0.3 mm in thickness were formed. The composition of the sample milled for 70 h was examined and found to contain 0.3% Cr contamination, originating from the abrasion of the vials and balls. HRTEM samples were prepared by the normal method which involves mechanical grinding, dimpling and ion beam milling. HRTEM observations and energy dispersive spectroscopy (EDS) analyses were performed in an HF-3000 field emission gun transmission electron microscope (FEG-TEM) with a point resolution of 1.9 Å and at an operating voltage of 300 kV. A beam size of about 2 nm and a typical spectrum collecting time of 100 s were used to the nanoscale EDS analyses.

All $\text{Fe}_{50}\text{Cu}_{50}$ samples with different milling times have been investigated by XRD. It is found that with increasing milling time the diffraction peaks of bcc phase reduce in intensity while increasing in width. In the sample milled for 30 h, Bragg peaks from both bcc and fcc phases can still be observed. After 70 h the bcc peaks completely disappear and only fcc peaks remain. The lattice parameter of the fcc phase increases from 0.3614(2) nm for the starting material to 0.3639(3) nm for the sample milled for 50 h and it remains unchanged with further milling. In the initial stage of the milling process (less than 20 h), the average crystallite size of both fcc and bcc phases is rapidly reduced to a constant value of approximately 15 nm. These results are consistent with data reported in Refs. 4–11.

Figure 1 shows a bright-field image, a dark-field image, and a corresponding electron diffraction pattern (EDP) of the sample milled for 30 h. It is found that grains are heavily strained and the grain size is not homogeneous but varies from 10 to 50 nm. Analyses of 50 grains showed that the average grain size is about 20 nm, which is slightly larger than that obtained from the XRD measurements. The EDP [Fig. 1(c)] from a larger region than that in Fig. 1(b) shows

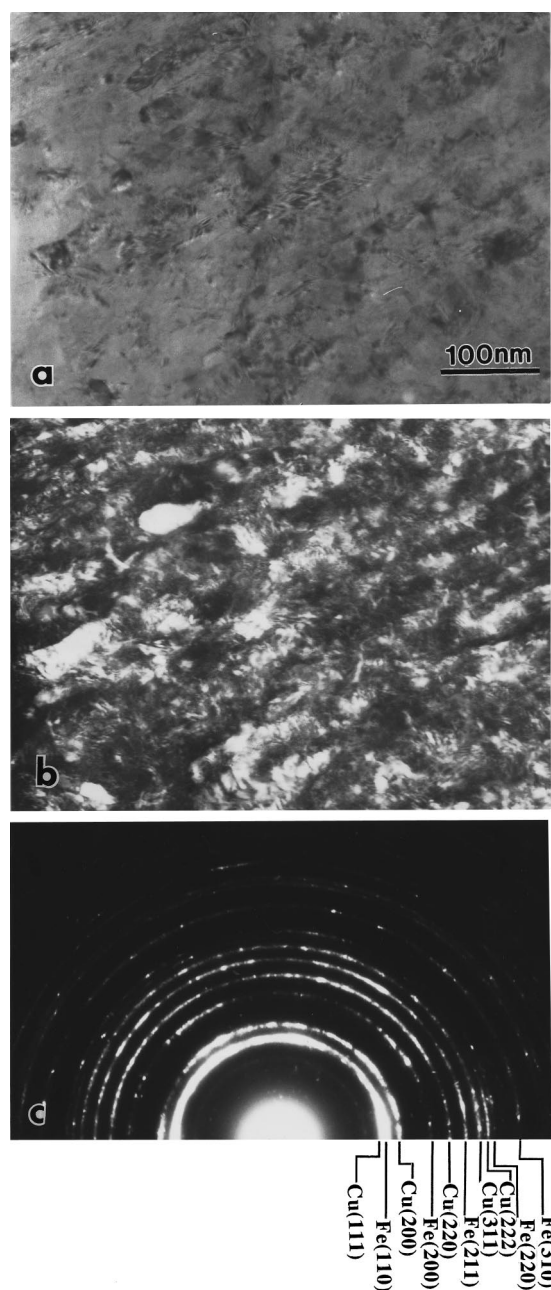


FIG. 1. TEM micrographs of $\text{Fe}_{50}\text{Cu}_{50}$ after 30 h of MA. (a) Bright-field image; (b) dark-field image, and (c) the corresponding EDP.

Debye-Scherrer rings and they can be indexed as those of fcc-Cu and bcc-Fe, respectively, which is in agreement with the XRD observation.

HRTEM images of bcc grains in the sample milled for 30 h are illustrated in Fig. 2. In a grain (~ 20 nm) having approximately $[001]$ zone axis [Fig. 2(a)] severe lattice distortion is clearly detected. The unit cell is distorted from a square shape to a rhombic one and the fourfold symmetry disappears. The deformation seems to be accommodated mainly by a simultaneous shear of all the atoms involved and the (110) planes in the upper part of the grain is tilted about 5° with respect to that of the lower part so that a low-angle grain boundary is generated. A number of edge dislocations with Burgers vector $\mathbf{b} = 1/2 [110]$ and slip planes of $\{110\}$

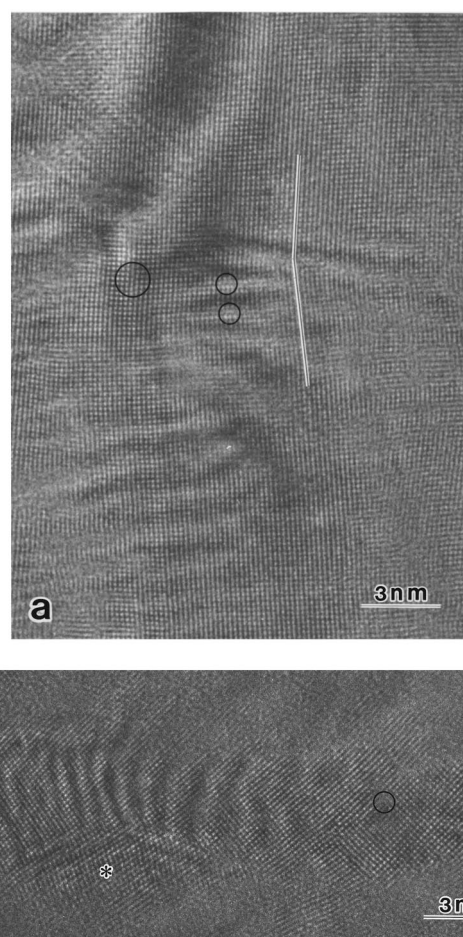


FIG. 2. HRTEM images of bcc grains in a $\text{Fe}_{50}\text{Cu}_{50}$ sample after 30 h of MA. (a) The white-edged black lines indicate a deviation of about 5° between the lower and upper part of the grain. The circles indicate some edge dislocations with $\mathbf{b} = 1/2 [110]$. (b) An elongated needlelike bcc grain. The circle and asterisk indicate a dislocation and a lattice distortion region, respectively.

were found near the low-angle grain boundary region. Dislocations and lattice distortion were also observed in smaller bcc grains, and an example is shown in Fig. 2(b). Composition analyses indicated that the Cu concentration was about 20 at. % in both small and large bcc grains. Interphase boundaries were frequently observed in specimens in the intermediate stage of milling. An HRTEM image of the sample milled for 30 h is illustrated in Fig. 3. The grain boundary is curved and slightly strained. A number of edge dislocations with Burgers vector $\mathbf{b} = 1/2 [110]$ were found in the fcc grain. The slip of these mobile dislocations are the main deformation mode in larger Cu grains, which was also observed in mechanically deformed copper.¹¹ The right-hand-side of the image is a bcc grain with a size of about 40 nm (only part of it is presented in Fig. 3), which aligns to nearly $[001]$ zone axis. Lattice distortion is not so severe in such larger grains as compared to that in smaller ones (cf., Fig. 2). Nanoscale composition analyses within the bcc grain indicated a higher mutual solubility near the interface region (~ 25 at. % Cu) than in the grain interior (~ 5 at. % Cu). This result suggests that mechanical deformation-induced diffusion is an important factor in controlling the alloying process. Further insight into such a deformation-induced diffu-

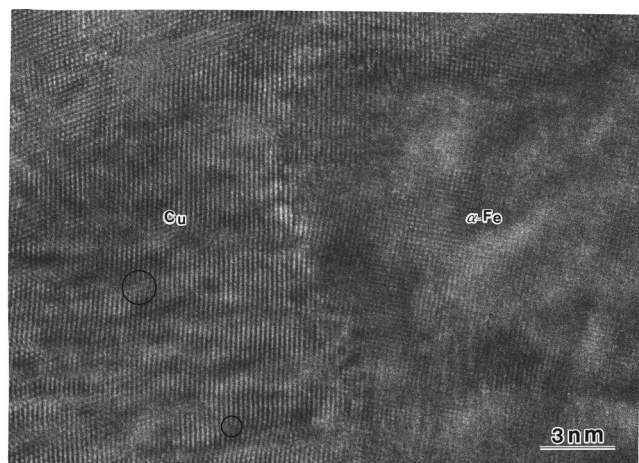


FIG. 3. An HRTEM image of an interface boundary in the sample milled for 30 h.

sion comes from recent Monte Carlo simulation results showing that atomic mixing may be a result of the kinetic process of continuous shearing of atom planes during milling-induced plastic deformation over phase segregation due to thermal diffusion.¹³ Monte Carlo simulations in the mean time show that with an increasing shearing frequency, such interfaces become increasing rough, leading to refinement of the microstructure and eventually to homogeneous mixing of the system. Another structural feature observed by HRTEM in specimens in the intermediate stage of milling is an interface structure as is illustrated in Fig. 4(a) together with the EDP's from both the upper grain [Fig. 4(b)] and the lower grain [Fig. 4(c)]. Both the lattice image and the EDP of the lower grain can be identified as $[00\bar{1}]_{\text{bcc}}$, while those of the upper grain can be identified as $[01\bar{1}]_{\text{fcc}}$. However, nanoscale composition analyses [Figs. 4(d) and 4(e)] revealed that both grains have a similar composition of $\text{Fe}_{80}\text{Cu}_{20}$. The Nishiyama-Wasserman (NW) orientation relationship, $[00\bar{1}]_{\alpha} \parallel [01\bar{1}]_{\gamma}$, and $(110)_{\alpha} \parallel (111)_{\gamma}$, was found, which is a typical orientation relationship held in the martensitic transformation. These results demonstrate that an α -to- γ $\text{Fe}_{80}\text{Cu}_{20}$ phase transformation (hereafter referred to: $\alpha \rightarrow \gamma$) has occurred during milling. Residual dislocations in fcc grains were found to be insignificant. The transformation seems to take place by a simultaneous shearing of all the atoms involved. This suggestion is further supported by the observation of some intermediate structures which resulted from shearing, as marked by asterisks in Fig. 4(a). The α/γ interface structure with the NW orientation relationship was also observed in other grains. The formation of the fcc- $\text{Fe}_{\text{rich}}\text{Cu}$ phase is also observed by Mössbauer studies.⁷ The $\alpha \rightarrow \gamma$ phase transformation occurring during the MA process might be explained by the following. It was predicted from CALPHAD calculations of the Fe-Cu system¹⁷ that the free energies of mixing for fcc and bcc structures are very similar in the composition range of $60 \leq x \leq 80$ at. %. This means that from thermodynamic viewpoint it could be possible that the grains with a composition of $\text{Fe}_{80}\text{Cu}_{20}$ have a fcc structure, as observed. Furthermore, the equilibrium phase diagram indicates that the $\alpha \rightarrow \gamma$ allotropic transformation temperature decreases from 912 °C to about 860 °C when 2% Cu is dissolved in the α -Fe lattice.¹⁸ The marten-

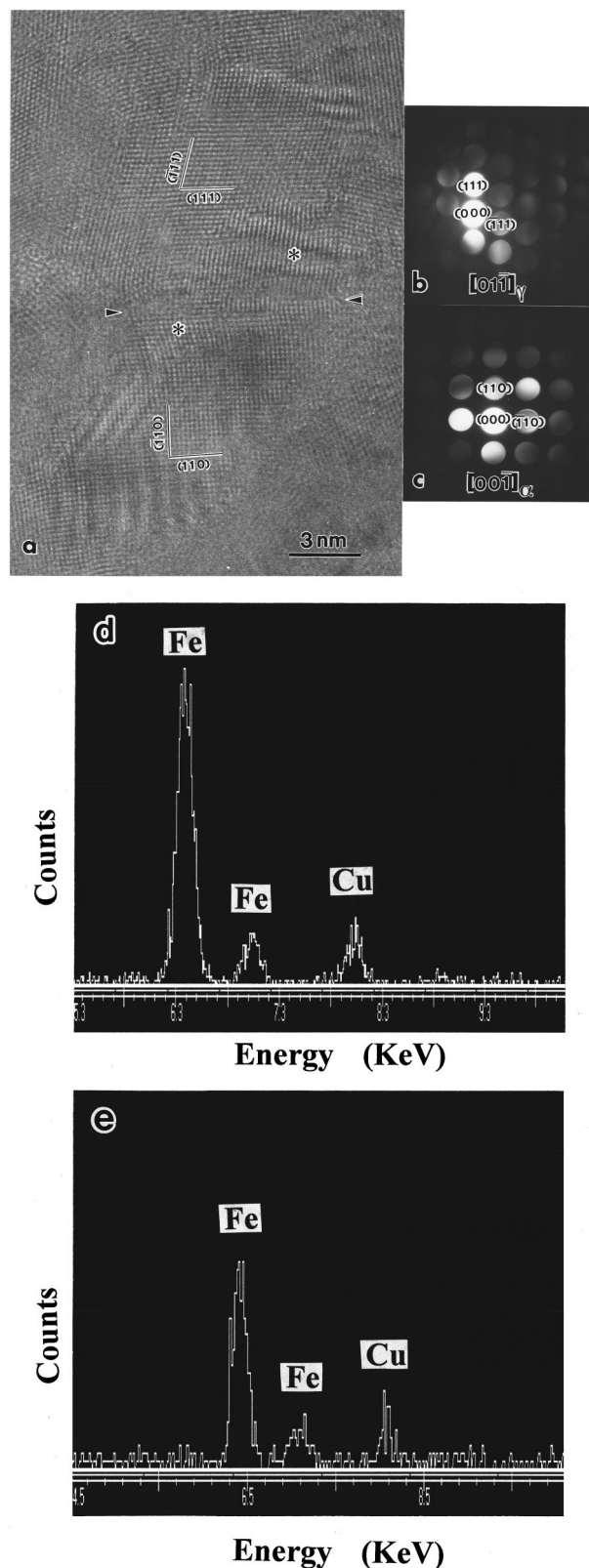


FIG. 4. An HRTEM image of an interface between bcc- and fcc- $\text{Fe}_{\text{rich}}\text{Cu}$ in the sample milled for 30 h, (a) The NW orientation relationships, i.e., $[00\bar{1}]_{\alpha} \parallel [01\bar{1}]_{\gamma}$, and $(110)_{\alpha} \parallel (111)_{\gamma}$, exist between the two phases. The arrows indicate the interface and asterisks mark lattice distortion regions. The EDP's and EDS from fcc- $\text{Fe}_{\text{rich}}\text{Cu}$ (top) and bcc- $\text{Fe}_{\text{rich}}\text{Cu}$ (bottom) are shown in (b), (d), (c), and (e), respectively.

sitic transformation temperatures (MTT) in bulk Fe-Cu alloys were also reported to decrease with increasing Cu content,¹⁹ e.g., MTT decreases from 650 °C to 540 °C when Cu content increases from 1% to 3.5%, respectively. By extrapolating the copper-content dependence of MTT and considering small grain sizes, it is not unreasonable to expect that MTT decreases to much lower temperatures in the supersaturated Fe_{rich}Cu solid solutions formed during milling, resulting in the $\alpha \rightarrow \gamma$ phase transformation.

Based on the results mentioned above and previous Mössbauer studies,⁷ we propose a possible mechanism of the alloying process in the Fe-Cu system from the kinetic viewpoint. Initially, the milling process reduces the crystallite sizes of both Fe and Cu powder blends to a few tens of nanometers due to the mobility of dislocations. Many defects, e.g., lattice distortion, dislocation, and low- and high-angle grain boundaries and interface boundaries, are formed in these nanostructured materials. This promotes the defect-induced interdiffusion processes, which has been indeed experimentally confirmed by Mössbauer measurements⁷ and the nanoscale composition analyses. In the former measurement, a nonmagnetic component (Fe diffuses into Cu) and a magnetic component (Cu diffuses into Fe) with an average hyperfine field of approximately 30 T were found in the samples at the intermediate milling stage, and in the latter analysis besides about 20% Cu content within Fe grains and 20% Fe content within Cu grains, a higher mutual solubility near the interface boundary region compared to that in the grain interior was also detected in the sample milled for 30 h. (Note that a chemical-driving diffusion reaction in the system with a positive heat of mixing generally results in decomposition of the alloy under equilibrium conditions.) The bcc-Fe_{rich}Cu grains which have MTT lower than the local

temperature at collisions with balls and vial become unstable and then the $\alpha \rightarrow \gamma$ phase transformation occurs by simultaneous shearing of the whole grain rather than by a dislocation mechanism due to the so-called "solid-solution softening" phenomena, which was indeed observed in nanocrystalline Fe_{rich}Cu prepared by ball milling.²⁰ On further increasing the milling time, although the average crystallite size of the fcc phases remains unchanged, interdiffusion between fcc-Fe_{rich}Cu and fcc-FeCu_{rich} is favored because of the similarity of the lattice structures. The last stage of milling is a homogenization process until a complete fcc-FeCu solid solution is formed.

In conclusion, HRTEM and EDS analyses show that the alloying process in the Fe-Cu system during milling is kinetically governed by the atomic shear effect and the shear-induced interdiffusion process. It is found that an $\alpha \rightarrow \gamma$ phase transformation occurs by simultaneous shearing process when the Cu content reaches 20 at. % in bcc-Fe_{rich}Cu grains with the grain size of about 20 nm. Further milling promotes the interdiffusion between fcc-Fe_{rich}Cu and fcc-FeCu_{rich}, which is favored because of the similarity of the lattice structures, until a complete fcc-Fe-Cu solid solution is formed. The investigations support recent Monte Carlo simulations showing that shearing overwhelming thermal diffusion is responsible for the mechanical alloying in Fe-Cu.¹³ The results presented here provide additional understanding in the formation of solid solution by mechanical alloying in systems with positive heat of mixing.

We wish to thank Professor S. Horiuchi and Professor Y. Matsui at the National Institute for Research in Inorganic Materials, Tsukuba, for the permission of free use of the HF-3000 FEG-TEM. This work was partly supported by the Danish Technical Research Council.

*Corresponding author; electronic address:

jyhuang@uhvem.osaka-u.ac.jp

¹See for example, *Proceedings of the International Symposium on Metastable Mechanically Alloyed and Nanocrystalline Materials*, 1995, edited by R. Schulz (Trans Tech Publications, Quebec, 1995); *ibid.*, 1996, edited by D. Fiorani and M. Magini (Trans Tech Publications, Rome, 1996); *ibid.*, 1997, edited by M. D. Baro and S. Surinach (Trans Tech Publications, Barcelona, 1997).

²W. L. Johnson, *Prog. Mater. Sci.* **30**, 81 (1986); C. C. Koch, in *Materials Science and Technology*, edited by R. W. Cahn, P. Haasen, and E. J. Kramer (VCH, Weinheim, 1991), Vol. 15, p. 193.

³E. Ma and M. Atzmon, *Mater. Chem. Phys.* **39**, 249 (1995); J. Z. Jiang *et al.*, *Mater. Sci. Eng. A* **242**, 268 (1998), and references therein.

⁴K. Uenish *et al.*, *Z. Metallkd.* **83**, 132 (1992).

⁵A. R. Yavari, P. J. Desre, and T. Beenameur, *Phys. Rev. Lett.* **68**, 2235 (1992); *Mater. Sci. Eng. A* **179/180**, 20 (1994); O. Drbohlav and A. R. Yavari, *J. Magn. Magn. Mater.* **137**, 243 (1994); *Acta Metall. Mater.* **43**, 1799 (1995).

⁶J. Eckert *et al.*, *J. Mater. Res.* **7**, 1980 (1992); *J. Appl. Phys.* **73**, 131 (1993); **73**, 2794 (1993).

⁷J. Z. Jiang *et al.*, *Appl. Phys. Lett.* **63**, 1056 (1993); **63**, 2768 (1993); *J. Phys.: Condens. Matter* **6**, L227 (1994); **6**, L343 (1994).

⁸P. Crespo *et al.*, *Phys. Rev. B* **48**, 7134 (1993); *J. Appl. Phys.* **76**, 6322 (1994); **39**, 249 (1995); A. Hernando *et al.*, *Europhys. Lett.* **32**, 585 (1995).

⁹E. Ma *et al.*, *J. Appl. Phys.* **74**, 955 (1993); P. J. Schilling *et al.*, *Appl. Phys. Lett.* **68**, 767 (1996); E. Ma *et al.*, *Phys. Rev. B* **55**, 5542 (1997).

¹⁰T. Ambrose *et al.*, *J. Magn. Magn. Mater.* **124**, 15 (1993).

¹¹J. Y. Huang *et al.*, *Nanostruct. Mater.* **4**, 1 (1994); *J. Mater. Res.* **11**, 2717 (1996); *J. Mater. Sci.* **31**, 4165 (1996); *Acta Mater.* **44**, 1211 (1996); **45**, 113 (1997); *J. Mater. Res.* **12**, 936 (1997).

¹²P. P. Macri *et al.*, *J. Appl. Phys.* **76**, 4061 (1994).

¹³P. Bellon and R. S. Averbach, *Phys. Rev. Lett.* **74**, 1819 (1995).

¹⁴T. Li *et al.*, *Phys. Rev. B* **52**, 1120 (1995).

¹⁵M. Angioloni *et al.*, *Microsc. Microanal. Microstruct.* **6**, 601 (1995); *Mater. Sci. Forum* **195**, 13 (1995); G. Mazzone and M. V. Antisari, *Phys. Rev. B* **54**, 441 (1996).

¹⁶*Handbook of Binary Phase Diagram*, edited by W. G. Moffatt (Genium, New York, 1984), Vol. 2.

¹⁷A. Jansson, Trita Mac 0304, *Mater. Res. Center KTH*, Stockholm, Sweden, 1987.

¹⁸*Binary Phase Diagram*, edited by T. B. Massalski (American Society for Metals, Ohio, 1986), p. 916.

¹⁹E. Räsänen, *Tekn. Lic. thesis*, Institute of Technology, Helsinki, 1967; C. Gente, M. Oehring, and R. Bormann, *Phys. Rev. B* **48**, 13 244 (1993).

²⁰M. Zhu and H. J. Fecht, *Nanostruct. Mater.* **6**, 421 (1995); T. D. Sheng and C. C. Koch, *Acta Mater.* **44**, 753 (1996).